

Synthesis, Structure and Magnetic Properties of New Layered Iron-Oxychalcogenide $\text{Na}_2\text{Fe}_2\text{OSe}_2$

J. B. He^a, D. M. Wang^a, H. L. Shi^b, H. X. Yang^b, J. Q. Li^b, and G. F. Chen^{a*}

^aDepartment of Physics, Renmin University of China, Beijing 100872, People's Republic of China and

^bBeijing National Laboratory for Condensed Matter Physics, Institute of Physics, Chinese Academy of Sciences, Beijing 100190, People's Republic of China

(Dated: August 17, 2018)

A new layered iron-oxychalcogenide $\text{Na}_2\text{Fe}_2\text{OSe}_2$ has been synthesized and structurally characterized by powder X-ray diffraction. The structure is formed by alternate stacking of the newly discovered $[\text{Fe}_2\text{OSe}_2]^{2-}$ blocks and double layers of Na^+ . Conductivity study shows that $\text{Na}_2\text{Fe}_2\text{OSe}_2$ is a semiconductor with activation energy of 0.26 eV. Magnetic susceptibility and heat capacity measurements reveal that an antiferromagnetic phase transition occurs at $T_N=73$ K. A broad maximum of magnetic susceptibility and a slow decay of the specific heat above T_N , arise as a result of two-dimensional short-range spin correlation.

PACS numbers: 61.66.Fn, 72.20.-i, 75.50.Ee

Low-dimensional magnetic systems have been a major subject of theoretical and experimental studies in recent years, due to their special physical properties and potential applications, such as high temperature superconductivity (HTSC)¹⁻⁵ and colossal magnetoresistance (CMR).⁶⁻⁹ The recent discovery of superconductivity in layered iron-pnictides has evoked a renewed interest in these low dimensional 3d transition-metal compounds.¹⁰⁻¹⁹ In this system, the T_c has become the highest among layered transition-metal-based compounds, except for the high T_c in cuprates. The full details of the mechanism for such high T_c superconductors are not yet completely understood. It is accepted that antiferromagnetic (AF) spin fluctuations may play some underlying role in the superconductivity.

In general, the crystal structures of high T_c cuprates are perovskite related structures, and the structural features are based on a two-dimensional square lattice sheets of CuO_2 .¹⁻³ The new type of superconducting iron-pnictides are based instead on conducting layers of edge-sharing $\text{FeAs}_4/\text{FeSe}_4$ tetrahedra.^{10,15-19} In most of those compounds the CuO_2 sheets or $\text{FeAs}_4/\text{FeSe}_4$ tetrahedra layers are interleaved by layers of rare earth (alkali- or alkaline-earth) cations blocking electrical conduction. These parent compounds are commonly AF-Mott-insulators or AF-semimetals, which can become a superconductor upon electron- or hole-doping. A lot of efforts have been put into searching for new materials with similar crystal structure. The transition-metal oxychalcogenide, $\text{La}_2\text{O}_2\text{Fe}_2\text{OSe}_2$, containing anti- CuO_2 type square planar layer, was originally reported to be an antiferromagnetic insulator ($T_N = 93$ K) by Mayer.²⁰ In this structure, Fe^{2+} is also four-coordinated by Se^{2-} (located above or below the center of $[\text{Fe}_{4/2}\text{O}_{4/4}]^{2+}$ square unit), formed an edge-shared octahedral unit $[\text{Fe}_2\text{OSe}_2]^{2-}$. The more recent band calculation indicated that $\text{La}_2\text{O}_2\text{Fe}_2\text{OSe}_2$ is a Mott insulator due to the narrowing of Fe d -electron bands and the enhanced correlation effects.²¹ This close structural relationship to iron-pnictides and cuprates make this system more

intriguing, and it is considered to be a good candidate for high T_c superconductor. Due to its fascinating structure and physical properties, a few new compounds, $(\text{Ba},\text{Sr})_2\text{F}_2\text{Fe}_2\text{OSe}_2$, with the same $[\text{Fe}_2\text{OSe}_2]^{2-}$ unit have been subsequently discovered, just using the fluorite type $[\text{Ba}_2\text{F}_2]^{2+}$ ($[\text{Sr}_2\text{F}_2]^{2+}$) block instead of the fluorite type $[\text{La}_2\text{O}_2]^{2+}$ block in $\text{La}_2\text{O}_2\text{Fe}_2\text{OSe}_2$. These new materials were found to order antiferromagnetically between 83-107 K and was proposed to be a rare example of a frustrated AF checkerboard spin lattice.²² We also noticed that a close-packed structure has been found in titanium oxypnictides $\text{Na}_2\text{Ti}_2\text{OP}_2$ ($P = \text{As}, \text{Sb}$),^{23,24} where the edge-shared $[\text{Ti}_2\text{OP}_2]^{2-}$ layers interspersed by double layers of Na^+ . The occurrence of a charge-density-wave- (CDW) or spin-density-wave-like (SDW) instability was reported from the electrical resistivity and magnetic susceptibility measurements, which are quite similar to the parent compounds of high T_c iron-oxypnictides.

Recently, we explored the range of such materials and discovered a new AF semiconductor $\text{Na}_2\text{Fe}_2\text{OSe}_2$, which is build by alternate stacking of $[\text{Fe}_2\text{OSe}_2]^{2-}$ blocks and double layers of Na^+ along c -axis. It is the first example of layered iron-oxychalcogenide with alkali metal. The temperature dependence of magnetic susceptibility and heat capacity shows that this material orders antiferromagnetically around $T_N = 73$ K and a two-dimensional (2D) short-range correlation persists up to temperatures of at least two times T_N .

Polycrystalline sample of $\text{Na}_2\text{Fe}_2\text{OSe}_2$ was synthesized by solid-state reaction method using Na (2N, lump), Se (5N, powder), Fe_2O_3 (3N, powder), and FeSe as starting materials. FeSe was prepared by reacting Fe powder with Se powder at 750 °C for 20 hours. Stoichiometric amount of Na lump, Se, FeSe and Fe_2O_3 powder were put into an alumina crucible and then sealed in quartz tube with Ar under the pressure of 0.4 atmosphere. The quartz tube was heated to 500 °C slowly and held there for 20 hours, and then cooled to room temperature naturally. In order to improve the homogeneity, the resulting product was then reground, pressed to a pellet, sealed in quartz tube

and reheated at 600 °C for a further 20 hours. Black single crystals could be obtained for annealing the mixture at elevated temperature of 700 °C over 200 hours. Except for heat-treatment, all manipulations for sample preparation were performed in glove boxes with a purified argon atmosphere.

The X-ray diffraction (XRD) data of $\text{Na}_2\text{Fe}_2\text{OSe}_2$ were collected at room temperature on a Bruker D8 advance using $\text{CuK}\alpha$ radiation (2θ range of 10-80°, a step width of 0.01° and a counting time of 2s). A low background, airtight specimen holder ring was used to avoid environmental effect. The XRD data were analyzed by the Rietveld method with Rietica 1.7.7 analysis package.²⁵ The Pseudo-Voigt (Riet asym) function was used as a profile function. The fixed background was applied by a cubic spline function. Isotropic atomic displacement parameters, B , with the isotropic Debye-Waller factor represented as $\exp(-B\sin^2\theta)/\lambda^2$ were assigned to all the sites. The resistivity was measured by a standard 4-probe method. The DC magnetic susceptibility was measured with a magnetic field of 1 T. The specific heat was measured by a standard calorimetric relaxation technique. These measurements were performed down to 2 K in a physical property measurement system (PPMS) of Quantum Design with the vibrating sample magnetometer (VSM) option provided.

TABLE I: Refined Structural Parameters for $\text{Na}_2\text{Fe}_2\text{OSe}_2$ at 300 K (Space Group $I4/mmm$ (No. 139); $Z = 2$; $a = 4.107(8)$ Å, $c = 14.641(8)$ Å, and $V = 247.07$ Å³, agreement factor $R_p = 3.52\%$, $R_{wp} = 7.43\%$, $R_{exp} = 2.10\%$, $S = 3.538$. The occupation (g) of all the sites is unity.)

atom	site	x	y	z	$B(\text{Å}^2)$
Na	4e	0	0	0.3363(8)	0.6110(2)
Fe	4c	0	1/2	0	0.1785(1)
Se	4e	0	0	0.1277(7)	0.5208(1)
O	2b	0	0	1/2	0.3316(2)

Figure 1(b) shows the X-ray diffraction pattern for an as-grown single crystal with the 00ℓ ($\ell = 2n$) reflections. The lattice constant $c = 14.67$ Å was calculated from the higher order peaks, comparable to the result from powder diffraction as described later. In Fig. 1(c) we present the energy dispersive x-ray microanalysis (EDX) spectrum taken on a piece of single crystal, which confirmed the presence of the Na, Fe, Se, and O elements. To determine the crystal structure, high quality powder XRD data were collected at room temperature, as shown in Fig. 1(a). The crystal structure of $\text{Na}_2\text{Ti}_2\text{OSb}_2$ ²³ in the space group $I4/mmm$ was used as a starting model for the final Rietveld refinement of the $\text{Na}_2\text{Fe}_2\text{OSe}_2$ structure. The refined structure parameters are summarized in table 1 and the crystal structure is illustrated in the inset of Fig. 1(a). The lattice parameters are determined to be $a = 4.107(8)$ Å and $c = 14.641(8)$ Å. $\text{Na}_2\text{Fe}_2\text{OSe}_2$ crystallizes in an anti- K_2NiF_4 type structure, built from alternate stacking of $[\text{Fe}_2\text{OSe}_2]^{2-}$ blocks and double layers

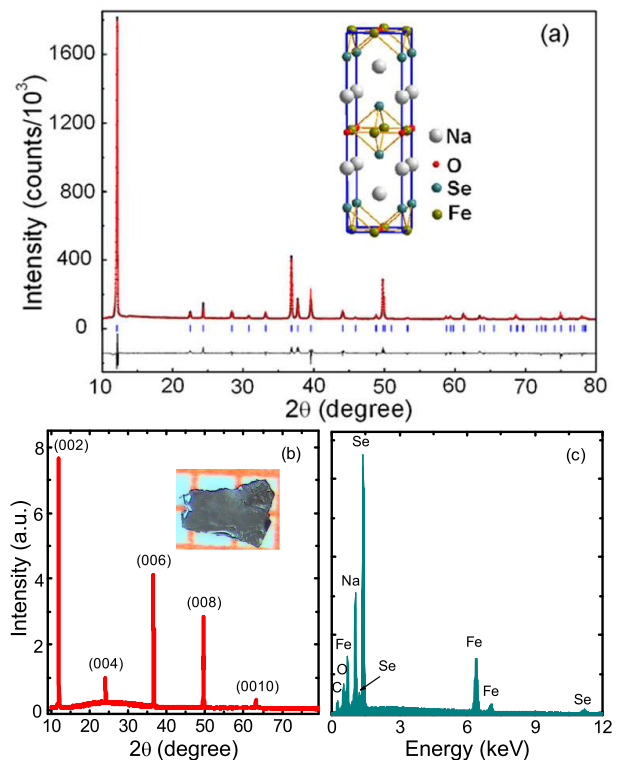


FIG. 1: (Color online) (a) Powder X-ray diffraction pattern at room temperature for $\text{Na}_2\text{Fe}_2\text{OSe}_2$. The solid line represents the intensities calculated using the Rietveld method. The bottom curves are the differences between the experimental and calculated intensities. The vertical lines indicate the Bragg peak positions of the target compound. The inset shows the crystal structure of $\text{Na}_2\text{Fe}_2\text{OSe}_2$. (b) Single crystal X-ray diffraction spectrum shows only the (00ℓ) reflections, indicating that the crystal is cleaved along the a - b plane. Inset: the picture of single crystal. (c) The EDX spectrum taken on a piece of single crystal.

of Na^+ along c -axis. In the $[\text{Fe}_2\text{OSe}_2]^{2-}$ unit, Fe^{2+} ion is located between oxygen atoms, forming a square-planar layer, $[\text{Fe}_{4/2}\text{O}_{4/4}]^{2+}$ (which is an anti-configuration to the $[\text{CuO}_{4/2}]^{2-}$ layer observed in high T_c cuprates), and two Se^{2-} ions are located above or below the center of $[\text{Fe}_{4/2}\text{O}_{4/4}]^{2+}$ square unit. In such layered compound, the inter-plane interaction is expected to be much weaker than the intra-layer one, which is beneficial to the formation of 2D magnetism and short-range correlation.

Figure 2 shows the temperature dependence of electrical resistivity measured for poly- and single-crystal samples of $\text{Na}_2\text{Fe}_2\text{OSe}_2$. Both of them show an insulating behavior. The overall resistivity of the polycrystal was nearly two orders higher than that of single crystal, which might be ascribed to the apparent grain boundary resistivity. The room temperature resistivity of $\text{Na}_2\text{Fe}_2\text{OSe}_2$ single crystal is about 500 Ωcm , comparable to the value observed for polycrystalline $\text{La}_2\text{O}_2\text{Fe}_2\text{OSe}_2$ (100 Ωcm).^{20,21} The electrical resistivity can be described by an Arrhenius temperature de-

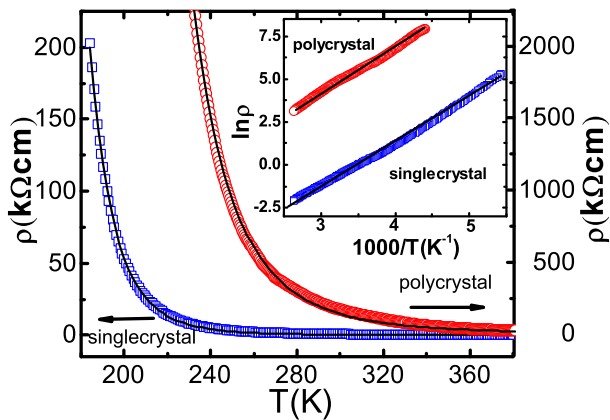


FIG. 2: (Color online) Temperature dependence of electrical resistivity for poly- and single-crystal samples of $\text{Na}_2\text{Fe}_2\text{OSe}_2$. Inset: The natural logarithm of electrical resistivity $\ln \rho$ plotted against reciprocal of temperature.

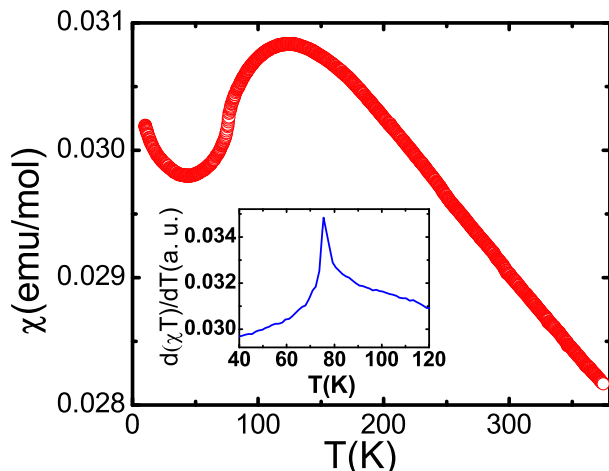


FIG. 3: (Color online) Temperature dependence of DC magnetic susceptibility measured at 1 T. The inset shows $d(\chi T)/dT$.

pendence, $\rho(T) = \rho_0 \exp(E_a/k_B T)$, where ρ_0 is a pre-exponential factor, E_a is the activation energy, and k_B is the Boltzmann constant. The activation energies E_a were estimated to be 0.26 eV and 0.24 eV for single- and poly-crystal, respectively, which are larger than that of $\text{La}_2\text{O}_2\text{Fe}_2\text{OSe}_2$ (0.19 eV).²¹ We attribute this difference to electron hopping between adjacent spin sites in such a magnetic semiconductor. Our Rietveld refinement results showed that it has longer $\text{Fe} \cdots \text{Fe}$, $\text{Fe}-\text{Se}$, $\text{Fe}-\text{O}$ distances for $\text{Na}_2\text{Fe}_2\text{OSe}_2$, therefore a lesser integral for hopping between adjacent Fe^{2+} sites was expected to account for the smaller electrical conductivity.

Figure 3 shows the temperature dependence of DC magnetic susceptibility measured at 1 T for polycrystalline $\text{Na}_2\text{Fe}_2\text{OSe}_2$, which shows a broad maximum around $T_{max} = 125$ K and a clear point of inflexion at $T_N = 75$ K. This anomaly is clearly seen in $d(\chi T)/dT$ (Inset of Fig. 3). The pronounced peak at T_N indi-

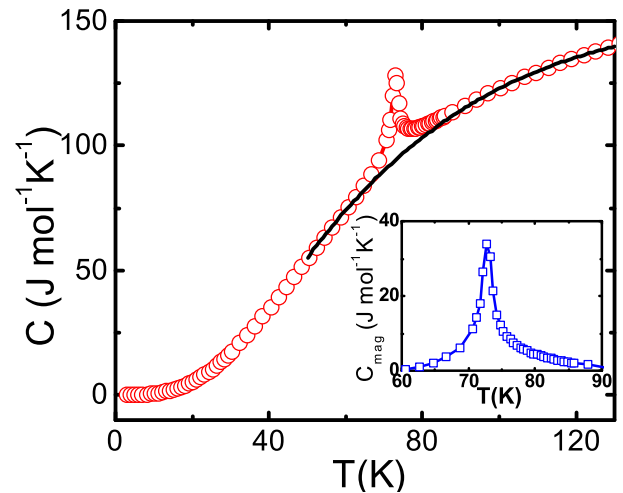


FIG. 4: (Color online) Heat capacity data measured for polycrystalline $\text{Na}_2\text{Fe}_2\text{OSe}_2$. The solid curve represents the lattice contribution, fitted by a polynomial. Inset: The estimated magnetic contribution.

cates the onset of a long-range AF ordering for $T < T_N$. Broadening of the susceptibility maximum and deviation from Curie-Weiss law even at high temperatures, indicate the strong AF short-range correlations, which is the characteristic behavior observed in many 2D magnetic systems. Usually, the ratio of T_N/T_{max} is often used to evaluate the extent of these low-dimensional magnetic correlations. Applying this simple criterion to our spin system ($T_N/T_{max} = 0.58$), it could be concluded that $\text{Na}_2\text{Fe}_2\text{OSe}_2$ is a typical 2D magnetic system. In general, in a layered magnetic compound, competition between intra-layer exchange interactions leads to the possibility of magnetic frustration effects. Indeed, a systemic studies on $(\text{Ba,Sr})_2\text{F}_2\text{Fe}_2\text{OSe}_2$ showed that these compounds have a frustrated checkerboard spin lattice.²² Similar effect was recently suggested also to play an important role in describing the magnetic structure of the isostructural $\text{La}_2\text{O}_2\text{Fe}_2\text{OSe}_2$.²⁶ Hence a shorter distance between $[\text{Fe}_2\text{O}]$ layers in $\text{Na}_2\text{Fe}_2\text{OSe}_2$ should enhance the frustration effect. A neutron experiment will provide more useful information to clarify this issue.

In order to further clarify the magnetic anomaly, we performed a heat capacity measurement. The temperature dependence of heat capacity C was plotted in Fig. 4. A clear λ -type shape of the C peak was observed at $T_N = 73$ K, which is due to a long-range antiferromagnetic ordering of the Fe^{2+} ion. The heat capacity tail due to short-range ordering of the 2D spin system can be seen more clearly above the transition temperature. The value of T_N determined from specific heat is somewhat lower than that one determined from DC magnetic susceptibility. The low temperature $C(T)$ curve is well fitted by a cubic term βT^3 . From the value of $\beta = 0.64 \text{ mJ mol}^{-1} \text{ K}^{-4}$, we estimate the Debye temperature $\Theta_D = 277$ K using the formula $\Theta_D = [12\pi^4 N R / (5\beta)]^{1/3}$. Because it is impossible to synthesize an analogous non-

magnetic crystal with the same structure to determine the correct lattice specific heat, we have to estimate the phonon contribution by fitting a polynomial to the C versus T curve at temperatures well away from T_N in the data, as shown in the inset of Fig. 4. By this rough approximation the magnetic contribution to the entropy over the entire temperature range ($S_{mag} = 2.4 \text{ Jmol}^{-1}\text{K}^{-1}$) seems too much smaller than the theoretical estimation for a completely ordered Fe^{2+} spin system ($S = R\ln 5 = 13.4 \text{ Jmol}^{-1}\text{K}^{-1}$). This shortfall of entropy implies that the background subtraction is not accurate enough to fully account for the short-range order entropy developed above T_N . This value is comparable to that of $\text{La}_2\text{O}_2\text{Fe}_2\text{OSe}_2$, in which the entropy release is less than 15% of $R\ln 5$.²⁷ We noticed that the features of C_{mag} and $d(\chi T)/dT$ (inset of Fig. 3) curves are in good qualitative agreement, due to the quantity of $d(\chi T)/dT$ being a direct representative of the magnetic contribution to the

heat capacity.

In summary, we have successfully synthesized the single- and poly-crystals of a new layered iron-oxychalcogenide $\text{Na}_2\text{Fe}_2\text{OSe}_2$, which have Fe_2O square planar layers with an anti- CuO_2 -type structure. The electrical resistivity, magnetic susceptibility and specific heat measurements indicated that this compound is a magnetic semiconductor and undergoes a long range AF magnetic transition below $T_N = 73 \text{ K}$. The broadening of the magnetic susceptibility and the slow decay process of the specific heat above T_N , indicate an extensive short-range order above the AF transition point. This behavior might be ascribed to the frustrated AF exchange interaction in such a 2D checkerboard spin lattice.

This work was supported by the Natural Science Foundation of China and the Ministry of Science and Technology of China.

-
- * Electronic address: genfuchen@ruc.edu.cn
- ¹ J. G. Bednorz, K. A. Müller, *Z. Phys. B: Condens. Matter* **64**, 189 (1986).
 - ² M. K. Wu, J. R. Ashburn, C. J. Torng, P. H. Hor, R. L. Meng, L. Gao, Z. J. Huang, Y. Q. Wang, and C. W. Chu, *Phys. Rev. Lett.* **58**, 908 (1987).
 - ³ Z. Z. Sheng, A. M. Hermann, *Nature* **332**, 138 (1988).
 - ⁴ C. C. Tsuei, J. R. Kirtley, Z. F. Ren, J. H. Wang, H. Raffy, Z. Z. Li, *Nature* **387**, 481 (1997).
 - ⁵ S. Sanna, G. Allodi, G. Concas, A. D. Hillier, and R. De Renzi, *Phys. Rev. Lett.* **93**, 207001 (2004).
 - ⁶ R. von Helmolt, J. Wecker, B. Holzapfel, L. Schultz and K. Samwer, *Phys. Rev. Lett.* **71**, 2331 (1993).
 - ⁷ A. Asamitsu, Y. Moritomo, Y. Tomioka, T. Arima and Y. Tokura, *Nature* **373**, 407 (1995).
 - ⁸ Y. Moritomo, A. Asamitsu, H. Kuwahara and Y. Tokura, *Nature* **380**, 141 (1996).
 - ⁹ J. M. D. Coey, M. Viret, L. Ranno, and K. Ounadjela, *Phys. Rev. Lett.* **75**, 3910 (1995).
 - ¹⁰ Y. Kamihara, T. Watanabe, M. Hirano, and H. Hosono, *J. Am. Chem. Soc.* **130**, 3296 (2008).
 - ¹¹ G. F. Chen, Z. Li, D. Wu, G. Li, W. Z. Hu, J. Dong, P. Zheng, J. L. Luo, and N. L. Wang, *Phys. Rev. Lett.* **100**, 247002 (2008).
 - ¹² X. H. Chen, T. Wu, G. Wu, R. H. Liu, H. Chen, and D. F. Fang, *Nature* **453**, 761 (2008).
 - ¹³ G. F. Chen and W. Z. Hu and J. L. Luo and N. L. Wang, *Phys. Rev. Lett.* **102**, 227004 (2009).
 - ¹⁴ Z. A. Ren, J. Yang, W. Lu, W. Yi, X. L. Shen, Z. C. Li, G. C. Che, X. L. Dong, L. L. Sun, F. Zhou, and Z. X. Zhao, *Europhys. Lett.* **82**, 57002 (2008).
 - ¹⁵ M. Rotter, M. Tegel, D. Johrendt, *Phys. Rev. Lett.* **101**, 107006 (2008).
 - ¹⁶ F. C. Hsu, J. Y. Luo, K. W. Yeh, T. K. Chen, T. W. Huang, P. M. Wu, Y. C. Lee, Y. L. Huang, Y. Y. Chu, D. C. Yan and M. K. Wu, *Proc. Nat. Acad. Sci.* **105**, 14262 (2008).
 - ¹⁷ X. C. Wang, Q. Q. Liu, Y. X. Lv, W. B. Gao, L. X. Yang, R. C. Yu, F. Y. Li, and C. Q. Jin, *Solid State Communications* **148**, 538 (2008).
 - ¹⁸ X. Y. Zhu, F. Han, G. Mu, P. Cheng, B. Shen, B. Zeng, and H. H. Wen, *Phys. Rev. B* **79**, 024516 (2009).
 - ¹⁹ J. G. Guo, S. Jin, G. Wang, S. Wang, K. Zhu, T. Zhou, M. He and X. L. Chen, *Phys. Rev. B* **82**, 180520 (2010).
 - ²⁰ J. M. Mayer, L. E. Schneemeyer, T. Siegrist, J. V. Waszczak, and B. Van Dover, *Angew. Chem., Int. Ed. Engl.* **31**, 1645 (1992).
 - ²¹ J. X. Zhu, R. Yu, H. Wang, L. L. Zhao, M. D. Jones, J. Dai, E. Abrahams, E. Morosan, M. Fang, and Q. Si, *Phys. Rev. Lett.* **104**, 216405 (2010).
 - ²² H. Kabbour, E. Janod, B. Corraze, M. Danot, C. Lee, M.-H. Whangbo, and L. Cario, *J. Am. Chem. Soc.* **130**, 8261 (2008).
 - ²³ T. C. Ozawa, R. Pantoja, E. A. Axtell III, S. M. Kauzlarich, J. E. Greedan, M. Bieringer, and J. W. Richardson, Jr., *J. Solid State Chem.* **153**, 275 (2000).
 - ²⁴ T. C. Ozawa, S. M. Kauzlarich, M. Bieringer, and J. E. Greedan, *Chem. Mater.* **13**, 1804 (2001).
 - ²⁵ B. A. Hunter, *Rietica. IUCR Powder Diffraction.* **22**, 21 (1997).
 - ²⁶ David G. Free and John S. O. Evans, *Phys. Rev. B* **81**, 214433 (2010).
 - ²⁷ Y. Fuwa, M. Wakeshima, and Y. Hinatsu, *J. Phys.: Condens. Matter* **22**, 346003 (2010).